

Magnet Design of a Proton and Carbon-ion Synchrotron for Cancer Therapy

Hyung-Suck SUH,^{*} Young-Gyu JUNG and Heung-Sik KANG[†]
Pohang Accelerator Laboratory, POSTECH, Pohang 790-784

(Received 24 November 2009, in final form 22 March 2010)

The magnets for a medical synchrotron for cancer therapy with proton and carbon-iron beams were designed. The synchrotron components are the magnetic septa, electrostatic septa, betatron core, and conventional magnets. This design was carried out to satisfy the physics requirements from the beam dynamics. We used a 3D code for the electromagnetic simulation and the optimization of the magnetic structures. In this paper, the basic design process for the electromagnetic devices will be described.

PACS numbers: 41.85.Ar, 41.85.Lc

Keywords: Cancer therapy, Synchrotron, Magnet design

DOI: 10.3938/jkps.56.1947

I. INTRODUCTION

Particle therapy using carbon ions has been highlighted for the past ten years worldwide because of its superior characteristics, such as high RBE (relative biological effectiveness) and small beam diffraction. Carbon-ion cancer therapy facilities using synchrotrons are being constructed in Europe and Japan. A synchrotron using a slow extraction scheme can provide the flexibility needed for dual species operation and for variable energy for active scanning of the particle beam onto a patient [1]. The disadvantage of a synchrotron is its big size and its complexity compared to a cyclotron, but its reliability and controllability are better than those of the cyclotron. Since a compact design for a synchrotron to reduce the construction cost is available, so far most carbon-ion cancer therapy facilities in use or under construction are synchrotron types.

A synchrotron accelerator for carbon ion cancer therapy needs to be compact, which can be accomplished by optimizing the lattice itself without losing performance. A medical synchrotron for carbon-ion cancer therapy is being designed to be compact for a hospital-based therapy facility [2,3]. The circumference of the synchrotron is only 60 meter, and the lattice is a FODO structure of 6 cells. Each cell has two dipole magnets with a bend angle of 30°. Figure 1 shows a schematic layout of the synchrotron in the course of design, and Table 1 lists the parameters of the designed lattice. The synchrotron facility consists of an ion source, which generates a proton or a carbon ion beam, a RFQ, an IH-linac, a synchrotron, and a transfer line to the gantry. The carbon

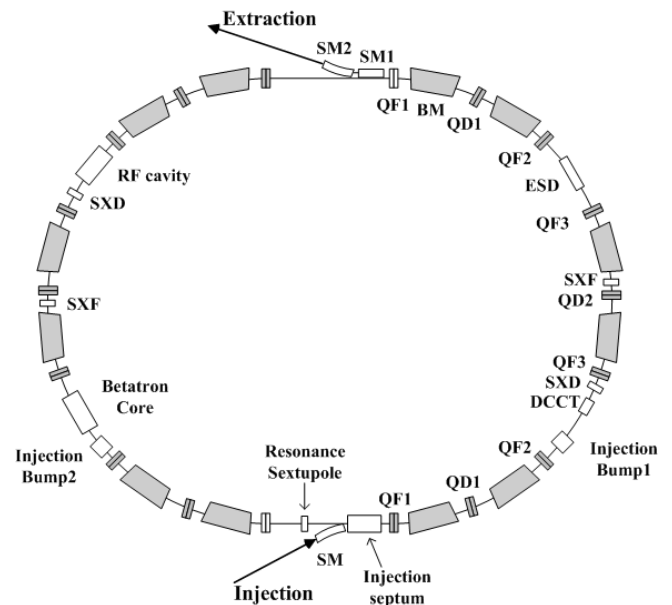


Fig. 1. Layout of the synchrotron (BM: dipole magnet, QF: quadrupole focusing, QD: quadrupole defocusing, ESD: electrostatic septum deflector, SXF: chromatic sextupole for the horizontal plane, and SXD: chromatic sextupole for the vertical plane).

ion from the ion source is $^{12}\text{C}^{+4}$, which is accelerated in the RFQ and the IH-linac to the injection energy and is then charge-stripped to $^{12}\text{C}^{+6}$ before injection to the synchrotron. In the synchrotron the beam is trapped, accelerated, and phase-jumped to increase the momentum spread, which is followed by a stabilizing start of spill and extraction. In the synchrotron, there should be dispersion-free straight sections in which septum mag-

^{*}E-mail: suhhs@postech.ac.kr; Fax: +82-54-279-1399

[†]E-mail: hskang@postech.ac.kr

Table 1. Parameters of the designed lattice.

Particle	Proton and Carbon ($^{12}C^{6+}$)
Extraction energy range	50 - 250 MeV for proton (3.5 - 38 cm) 85 - 430 MeV/u for carbon (3.5 - 38 cm)
Beam intensity	5×10^{10} ppp for proton 4×10^9 ppp for carbon
Magnetic rigidity	6.639 T-m
Dipole bending radius	4.76 m
Tune (Q_x, Q_y)	1.68 / 1.13
Injection energy	7 MeV/u
Max. β_x / β_y	11.1 / 19.4
Maximum dispersion, D_x	5.8 m
Circumference	60 m
Harmonic number	3
RF frequency	1.6 - 10.2 MHz
Operation cycle	
Injection and acceleration	500 ms
Flat-top (extracted spill duration)	1000 ms
fall	500 ms
Momentum acceptance	$\pm 0.5\%$
Max. repetition rate	0.5 Hz for carbon 1 Hz for proton
Extraction	third-integer resonance ($Q_x = 5/3 = 1.66666$) Betatron core, quadrupole driven Two electrostatic deflectors: < 80 kV/cm Two magnetic Septa: 0.5 T and 1.5 T 4 - 10 mm - multi-turn injection - thin electrostatic septum: deflection angle 7.5° - Electrode voltage : 112 kV - Three fast ramped bumper magnets 160 mm \times 7 mm
Beam diameter	
Injection	
Vacuum chamber aperture $h \times v$	
Injected beam enittance (rms) hor/ver	1π mm-mrd, 1π mm-mrad
RF cavity	Quarter-wave ferrite-loaded coaxial line Rf voltage: 5 kV Shunt impedance: 590 Ω RF power: 11 kW
Accelerating time	Ramping time: < 1 s Extraction time: 1 - 10 sec
Transition energy	1.968

nets for injection and extraction, a resonance sextupole, and a RF cavity are located.

II. BEAM DYNAMICS DESIGN

Multi-turn injection is chosen to provide proton or light ion beams with the intensity required for hadron therapy. An advantage of multi-turn injection is that

the accumulation of several injections allows the reduction of the required linac peak current from the required single-turn value by a factor equivalent to the number of effective injections. These are of the order of 5 or 6 if a practical efficiency of about 50% is assumed. The beam energy from the linac is 20 MeV for protons and 7 MeV/u for carbon ions.

Extraction is the most critical part in the design of a medical synchrotron. The slow beam extraction method from the synchrotron is a third-integer resonant scheme

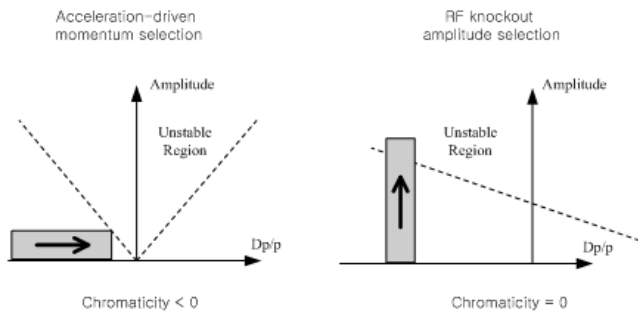


Fig. 2. Third-order resonance for extraction ($Dp/p = \Delta p/p$, momentum difference). The shaded box represents the particle beam. As the particle momentum is increased by the betatron core, the particle beam approaches the unstable region.

driven by sextupoles. The techniques for applying resonant extraction to achieve a long spill (seconds) can be classified into two groups, those that move the resonance (quadrupole-driven extraction) by changing the tune with quadrupoles and those that move the beam (acceleration-driven extraction, RF knockout extraction) (see Fig. 2). The latter has the advantage of keeping all lattice parameters and, hence, the resonance conditions constant.

The quadrupole-driven extraction scheme is to move the resonance line to a stationary beam by changing the tune close to the 3-rd order resonance with quadrupoles during the extraction, which is an easy way for extraction but results in an unavoidable movement of the beam at the septum for extraction. Thus, on-line orbit and focusing corrections are necessary in this scheme. In this scheme, if the betatron tune ν_x approaches slowly a third-order resonance $3\nu_x = l$ with integer l , beam particles can be slowly squeezed out of the stable area and extracted by using the next septum magnet.

The acceleration-driven extraction scheme is to move the beam into a stationary resonance by accelerating the beam. It doesn't need to change the tune so that the transverse optics of the ring can be kept constant through the extraction, which means there is no movement of the orbit or the extraction separatrices. It can offer smooth spill in the extraction, which is why this method is preferred for slow extraction. The beam acceleration can be done by using a betatron core or a stochastic noise system. As the particle momentum is increased by the betatron core, the particle beam approaches the unstable region, as shown in Fig. 2.

In this synchrotron lattice design, the acceleration-driven extraction scheme using the betatron core is chosen because it offers the smoothest spill of particles. As an alternative, the quadrupole-driven extraction scheme will be also prepared because it does not need any additional equipment. Using a betatron core enables control of both the length and the intensity of the spill. When an induction circuit is used, the betatron core accelerates

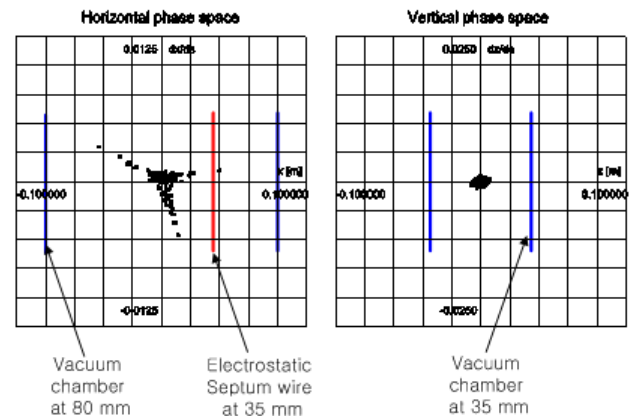


Fig. 3. Beam dynamics simulation result of 3rd order resonance extraction and the location of the electrostatic septum wire at ESD. The horizontal phase space shows a typical pattern of a 3rd order resonance. The deflecting electric field is applied between the electrostatic septum wire and the right chamber wall.

the waiting ion beam into the resonance. The betatron core is a smooth high-inductance device, compared to the small quadrupole lenses that are normally used to move the resonance, and is, therefore, better suited for delivering a very smooth spill.

Extraction starts from the ESD (electrostatic septum deflector), which is followed by the SM1 (thin septum) and the SM2 (thick septum) (see Fig. 1). Figure 3 shows the beam dynamics simulation of 3rd order resonance extraction and the location of the electrostatic septum wire at ESD, 35 mm from the center, where the particle that deviates horizontally from the orbit center due to 3rd order resonance receives an electrostatic kick to enter the field region of the SM1. The horizontal phase space shows the typical pattern of a 3rd order resonance. The deflecting electric field is applied between the electrostatic septum wire and the right chamber wall.

III. MAGNET DESIGN

The conventional magnet system is composed of 12 bending magnets, 18 quadrupoles, 4 sextupoles, and 1 resonance sextupole. Their poles are shaped to minimize the integrated errors, as individual requirements [4]. The main devices for injection and extraction are the magnetic septa and the electrostatic septa. The betatron core increases the beam energy to be extracted with the resonant sextupole. The electromagnetic simulations for the magnet design are done with OPERA/TOSCA and ELEKTRA. The design features of the magnets will be described in detail. Table 2 lists the requirements for the magnets.

Table 2. Requirements of the magnets.

	Magnetic field [T, T/m, T/m ²]	effective length [m]	Bending angle	Pole gap, aperture diameter [m]	Good field region	Field uniformity
Dipole	1.5	2.2	30	0.07	±60 mm	<±2 × 10 ⁻⁴
Quadrupole	6	0.35		0.15	±60 mm	<±5 × 10 ⁻⁴
Sextupole	35	0.3		0.2	±60 mm	<±4 × 10 ⁻⁴
Sextupole (Resonance)	80	0.3		0.2	±60 mm	<±4 × 10 ⁻⁴

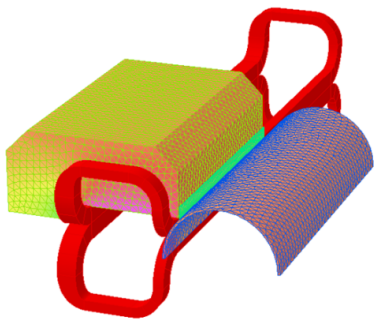


Fig. 4. (Color online) FEM model (a quarter) of the injection septum due to symmetry. A field shield plate (green part) is used to decrease the field at the stored chamber (blue part).

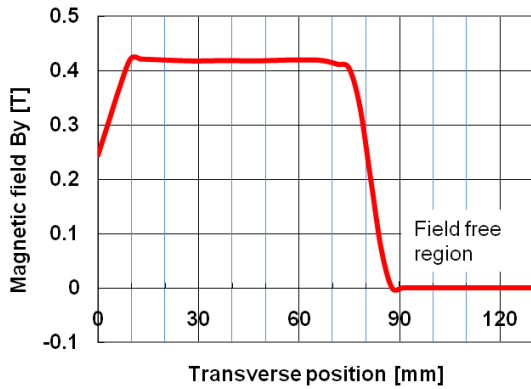


Fig. 5. Magnetic field distribution of the injection septum on the midplane. FEM results show about 1 Gauss in the field-free region with a 1-mm shield plate.

1. Magnetic Septa

Magnetic septa are used for injection and extraction, as shown in Table 3. These septa will be DC and will only be changed when the particle species or the particle energy are changed. Their cores have a C-type configuration and are laminated. To reduce the leakage field in the adjacent bypass channel to as low as possible, we made the pole shallow. Figure 4 shows a FEM model of injection magnetic septum. A field shield plate will be used

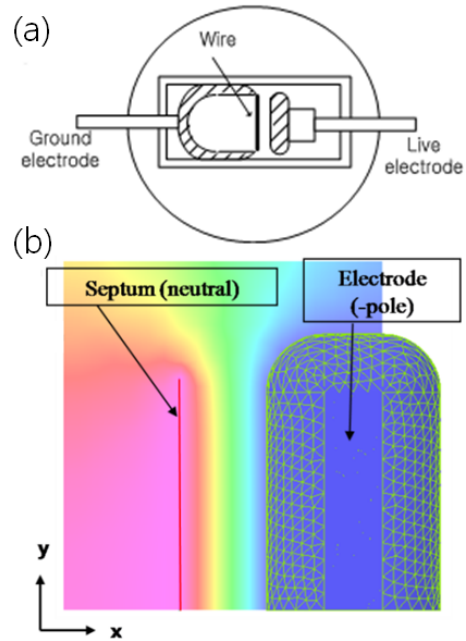


Fig. 6. (Color online) (a) Cross-sectional view and (b) potential contours of the electrostatic extraction septum. The main structure is made of stainless steel, but the septum wall is formed of tungsten wires.

to reduce the field at the stored chamber. The vertical magnetic field of the injection septum on the midplane is plotted in Fig. 5, which shows about 1 Gauss in the field-free region when a 1-mm shield plate is used.

2. Electrostatic Septa

An electrostatic injection septum deflects the beam from the linac at an angle of 60 mrad. Another electrostatic septum deflector (ESD in Figure 1) is used for beam extraction with the betatron core. Table 4 shows the differences between the electrostatic septa. From the equation of motion, we can estimate the required electric field. For the extraction electrostatic septum, the magnetic rigidity for a carbon ion of 430 MeV/u is 6.65 Tm, the required bending angle is 5.9 mrad, the effec-

Table 3. Characteristics of the magnetic septa.

	Injection Septum	Extraction Thin Septum	Extraction Thick Septum
Effective length [m]	0.450	0.680	1.024
Yoke length [m]	0.413	0.641	0.978
Maximum field [T]	0.426	0.489	0.973
Deflection angle mrad	250	50	150
Temperature rise [°C]	5	9	12

Table 4. Parameters of the electrostatic septa.

	Injection ES	Extraction ES
Effective length [m]	0.6	1.0
Max. electric field [MV/m]	2.8	8.6
Deflection angle [mrad]	60	5.9

Table 5. Parameters of the dipole magnet.

Magnetic field	1.5 T
Effective length	2.2 m
Yoke length	2.074
Weight	10.5 tons
Bending angle	30°
Pole gap	70 mm
Good field region	±60 mm
Field uniformity	$< \pm 2 \times 10^{-4}$
Power	41 kW
Pressure drop	6.5 bar
Temperature rise	13 °C

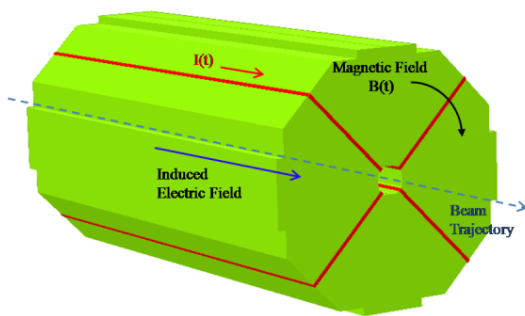
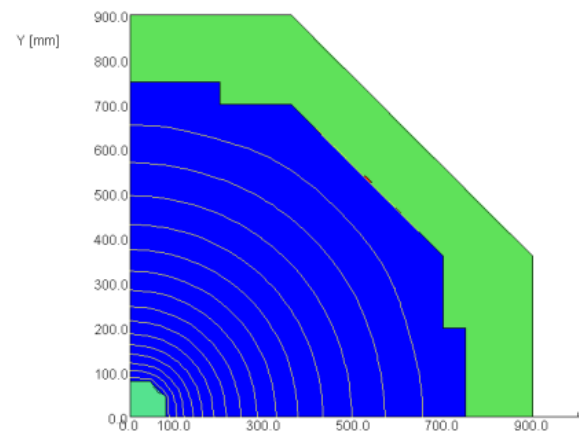


Fig. 7. Schematic view of the betatron core that changes its current level during extraction. Its yoke is made of laminations without causing excessive eddy-current power losses.

tive length is 1.0 m, so the required electric field is 8.6 MV/m. The potential contours of the electrostatic extraction septum based on the FEM are shown in Fig. 6. The main structure of the ESD is made of stainless steel, but the septum wall is formed of tungsten wires.

Table 6. Principle parameters of the sextupole magnets.

Parameters	Main Sextupole	Resonance Sextupole
Field gradient [T/m ²]	35	80
Effective length [mm]	300	300
Yoke length	172	72
Aperture radius [mm]	75	75
Good field radius [mm]	60	60
Multipole harmonic	$< \pm 4 \times 10^{-3}$	$< \pm 4 \times 10^{-3}$
Power [kW]	813	3317
Temperature rise [°C]	3	10

Fig. 8. Magnetic flux lines inside the betatron core. The variation in the kinetic energy caused by the betatron is $dE = Ze d\phi/dt$, where ϕ is the magnetic flux.

3. Betatron Core

A change in magnetic flux causes electromagnetic induction. Using this, a betatron core increases the beam energy to be extracted smoothly. The spill rate can be adjusted by using the betatron. We should elaborately calculate the magnetic flux change, including the eddy current and the nonlinear effects. The equations of the betatron are as follows: The variation of the kinetic energy caused by the betatron is $dE = Ze d\phi/dt$, where ϕ is the magnetic flux. Figure 7 shows a schematic view of the betatron core, and Figure 8 shows the magnetic flux lines inside core. The yoke of the betatron core is made of

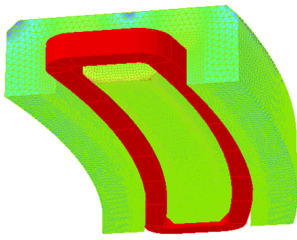


Fig. 9. FEM model (1/2) of the dipole magnet, an H-type cross section with a curved yoke to account for the 151-mm beam sagitta.

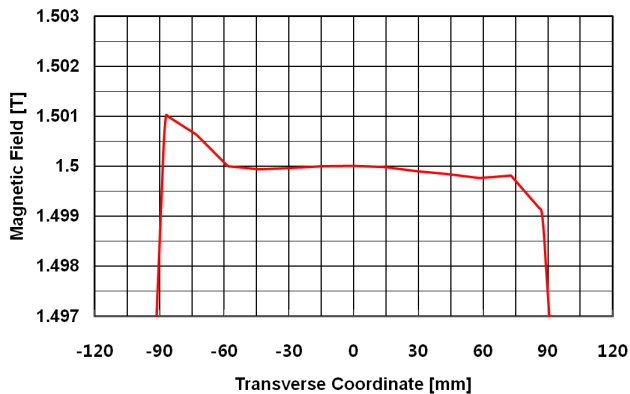


Fig. 10. Field uniformity of the dipole magnet. $\Delta B/B < \pm 2 \times 10^{-4}$ for the ± 60 -mm transverse range.

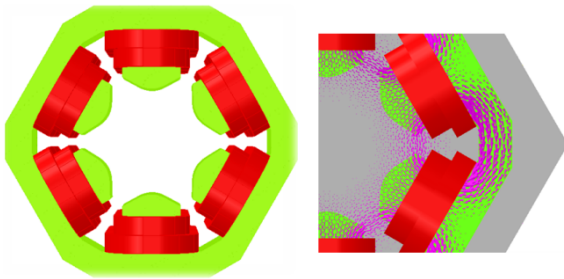


Fig. 11. FEM model of the sextupole and its flux profile. Sextupoles are required for the chromaticity correction and for resonant extraction.

laminations without causing excessive power losses due to eddy current.

4. Dipole Magnet

The yoke of the dipole magnet has an H-type shape for good field uniformity and is curved to reduce the volume.

The nominal magnetic field is 1.5 T, and the gap height is 70 mm. The poles have been optimized to reach the required homogeneity. The FEM model of the magnet is shown in Fig. 9, and the homogeneity of the field ($< \pm 2 \times 10^{-4}$ for $x: \pm 60$ mm) is presented in Fig. 10. The main parameters are summarized in Table 5.

5. Sextupole Magnet

Sextupoles are required for chromaticity correction and for resonant extraction. The two kinds of sextupoles have the same core, but different coil size and turn number. Figure 11 shows the FEM model and the flux profile of the sextupole. The major parameters are summarized in Table 6.

IV. SUMMARY

The first conceptual design of magnets for a medical synchrotron has been performed, but we should investigate the field profile of the magnets for the cases of low- and high-energy operation. Particularly, the beta-tron core needs many transient calculations to obtain a constant flux change.

ACKNOWLEDGMENTS

This work was supported by the Nuclear Research & Development Program of the Korea Science and Engineering Foundation (KOSEF) funded by the Korean government (MEST) (Grant code: M20090062 474).

REFERENCES

- [1] *Proton-Ion Medical Machine Study (PIMMS) Accelerator Complex Study Group*, CERN/PS 99-010.
- [2] H. S. Kang, J. Y. Huang and J. H. Choi, *J. Korean Phys. Soc.* **53**, 544 (2008).
- [3] H. S. Kang and H. S. Suh, in *Proceedings of the European Particle Accelerator Conference 2008* (Genoa, Italy), p. 1803.
- [4] Jack T. Tanabe, *Iron Dominated Electromagnets* (World Scientific Pub. Ltd., Singapore, 2005) p. 19.